photonics

MDPI

Article

Performance Analysis of a Multi-Hop Parallel Hybrid FSO/RF System over a Gamma–Gamma Turbulence Channel with Pointing Errors and a Nakagami-*m* Fading Channel

Yan Wu [1], Jing Chen [2], Jianzhong Guo [1], Gang Li [1] and Dejin Kong [1,*]

[1] The State Key Laboratory of New Textile Materials and Advanced Processing Technologies, School of Electronic and Electrical Engineering, Wuhan Textile University, Wuhan 430200, China
[2] The Electronic Information School, Wuhan University, Wuhan 430200, China
* Correspondence: djkou@wtu.edu.cn

Abstract: Due to the influence of the atmospheric environment and pointing errors, the performance of free space optical communication is greatly limited. In this paper, we propose a parallel multi-hop hybrid free space optical (FSO)/radio frequency (RF) system to improve the system performance. The FSO sub-link and RF sub-link are modeled by Gamma–Gamma turbulence with pointing errors and Nakagami-m distributions, respectively. Based on the selective combination scheme, the probability density function (PDF) and cumulative distribution function (CDF) of the output signal-to-noise ratio (SNR) of the hybrid FSO/RF one-hop or direct link are obtained. Then, the PDF and CDF of the output SNR of the parallel multi-hop hybrid system are derived with the decoded forward (DF) protocol considered. Finally, the expressions of the average bit error rate (ABER) and outage probability are derived for the parallel multi-hop hybrid system, the hybrid FSO/RF direct link, and the FSO-only direct link. The results show that the parallel multi-hop hybrid system can effectively mitigate the negative impact of atmospheric turbulence and pointing errors and can significantly improve the system performance.

Keywords: multi-hop parallel hybrid FSO/RF system; gamma-gamma turbulence; nakagami-m fading; pointing errors; average bit error rate; outage probability

Citation: Wu, Y.; Chen, J.; Guo, J.; Li, G.; Kong, D. Performance Analysis of a Multi-Hop Parallel Hybrid FSO/RF System over a Gamma–Gamma Turbulence Channel with Pointing Errors and a Nakagami-*m* Fading Channel. *Photonics* **2022**, *9*, 631. https://doi.org/10.3390/photonics9090631

Received: 1 August 2022
Accepted: 30 August 2022
Published: 2 September 2022

1. Introduction

In recent years, due to its high capacity, license-free spectrum, fast network construction, and other characteristics, free space optical (FSO) communication is often considered as an ideal solution for the "last mile of telecommunications" and local area network (LAN) links between buildings as well as a potential next-generation wireless communication technology [1,2].

However, the performance of FSO communication is greatly affected by the atmospheric environment. For example, atmospheric turbulence will lead to scintillation effects, beam wandering and dispersion, bad weather (fog, rain, clouds, and snow) will lead to the attenuation of optical power, and the thermal expansion of the building causes sway, which makes the beam misalignment between the transmitter and the receiver. These all lead to the deteriorating performance of the FSO communication system [3].

Therefore, scholars from various countries have proposed various solutions to the problems faced by FSO communication systems. For example, the alignment of satellites and ground stations can be realized by acquisition, tracking, pointing (ATP) technology in satellite ground laser communication system [4]. Adaptive optics can be used to compensate for the negative impact of turbulence on the performance of the FSO system [5]. For the FSO system operating in bad weather, the beam with the wavelength of the atmospheric window can be used as the carrier, and a beam with excellent performance can also be selected to transmit information [6].

For the more complex and fast time-varying communication environment, the hybrid FSO and radio frequency (RF) link can be used to mitigate the impact of this environment on the system, so as to improve the performance of the communication system [7]. In order to realize the long-distance transmission and wide coverage of free space optical communication, the multi-hop transmission mode is considered as an effective solution [8–10]. The performance of the FSO system may be further improved by adopting some common communication technologies, such as diversity technology (time diversity, space diversity, and wavelength diversity) [11,12], modulation technology (on-off keying modulation, pulse position modulation, and subcarrier modulation) [13–15].

Currently, the FSO link has the advantage of large transmission capacity and the RF link is less affected by the environment. The hybrid FSO/RF system, which combines the advantages of the FSO and RF links, can greatly improve the communication performance; therefore, it has been widely studied by researchers. The hybrid system can generally be divided into hard switching and soft switching.

In the hard switching system, the RF link, as an alternative, can only be enabled when the FSO link is blocked and channel-state-information (CSI) needs to be provided [16–18]. Makki et al. [19] deduced the closed-form expressions of throughput and outage probability of the hybrid system (RF link was used as a backup link at this time) considering the presence and absence of hybrid automatic retransmission request (HARQ). In the soft switching system, the FSO link and RF link transmit the same information at the same time, and the received signal is processed by different combination schemes at the receiver, which does not need to provide CSI [20–22]. Shakir et al. [23] proposed a hybrid system based on the selective combination scheme and derived new closed-form expressions for the average bit error rate (ABER) and outage probability of the system under turbulent conditions.

When the transmission distance exceeds 1km, the performance of the FSO communication system will deteriorate sharply due to environmental impact [24]. Therefore, for the needs of long-distance transmission and coverage expansion, increasingly scholars have conducted research on multi-hop relay networks based on FSO. The multi-hop relay network is divided into serial multi-hop relay and parallel multi-hop relay.

The serial multi-hop relay is a multi-hop relay transmission mode, which includes amplify-and-forward (AF) transmission and decode-and-forward (DF) transmission [25–28]. Zedini et al. [26] analyzed the performance of the multi-hop FSO communication system with AF relay and CSI assistance, and derived mathematical expressions of the end-to-end communication performance of the system under the Gamma–Gamma turbulence with pointing errors, such as the ABER and ergodic channel capacity. Amirabadi et al. [28] proposed and analyzed two novel serial multi-hop relay-assisted hybrid FSO/RF communication systems.

The multi-hop parallel relay is a multi-hop cooperative diversity transmission mode [29,30]. Kashani et al. [31] proposed a parallel multi-hop FSO communication system and derived the outage probability expression of the system under the Log-Normal turbulence environment. The simulation results show that the parallel multi-hop FSO communication system can significantly improve the communication performance compared with the serial or parallel relay scheme. Wang et al. [32] deduced the mathematical expressions of the ABER and outage probability of the parallel multi-hop FSO communication system with the DF protocol and the Exponentiated Weibull (EW) turbulence. Furthermore, the effects of different turbulence intensity, receiver aperture size and different hops on the ABER performance of the system were further analyzed.

Thus, motivated by the above mentioned facts and considering its military and disaster recovery applications, in this paper, we propose a new multi-hop parallel hybrid communication scheme combining the hybrid FSO/RF parallel transmission mode and the multi-hop parallel relay-aided communication mode—that is, the multi-hop parallel hybrid FSO/RF system.

The hybrid FSO/RF parallel transmission mode has the advantages of both the large capacity of the FSO sub-link and the reliability of the RF sub-link. And the multi-hop parallel relay-aided communication mode has the advantages of wide coverage, long transmission distance and strong disaster recovery capability. Therefore, the multi-hop parallel hybrid FSO/RF communication system has better communication performance, higher reliability, wider coverage, longer transmission distance and stronger recovery capability. Then, the performance of the multi-hop parallel hybrid system is analyzed. The major contributions of our work are as follows:

- We first propose a multi-hop parallel hybrid FSO/RF communication system. The communication system with this structure has not been reported in the existing literature.
- The PDF and CDF of the output SNR of the parallel multi-hop hybrid system are derived with the DF protocol considered. The FSO sub-link experiences the Gamma–Gamma turbulence with pointing errors, and the RF sub-link suffers Nakagami-m fading channel.
- Through the analysis of communication performance, the new expressions of the end-to-end ABER and outage performance of the multi-hop parallel hybrid FSO/RF system, the hybrid FSO/RF direct link and the FSO-only direct link are derived.
- The effects of different modulation modes, different turbulence intensities, different pointing errors, different RF fading channels and different relay-aided structures on the performance of the multi-hop parallel hybrid system, the hybrid FSO/RF direct link and the FSO-only direct link are compared and analyzed.

The remainder of the paper is structured as follows. In Section 2, the multi-hop parallel hybrid FSO/RF link system model is presented, and the statistical characteristics of the FSO sub-link, the RF sub-link, and the hybrid FSO/RF one-hop link are described. The end-to-end performance expressions of the multi-hop parallel hybrid system are derived in Section 3. Numerical results and discussions are provided in Section 4, and finally, our concluding remarks are summarized in Section 5.

2. System and Channel Model

The schematic of the multi-hop parallel hybrid FSO/RF cooperation system is shown in Figure 1. For a multi-hop parallel hybrid system with (N, M) structure, the source digital signal has $N + 1$ paths and each cooperation path has M hops from the source node to the destination node—that is, there is a direct path from the source node to the destination node and N cooperation paths, where each cooperation path has M hops branches (include $M - 1$ relays in each path).

In each one-hop link or direct link, the source digital signal is divided into two identical signals after subcarrier modulation. These two modulated signals are loaded onto the carriers by FSO and RF transmitters, respectively. In each regenerative repeater, the signal with the maximum SNR from the two received signals is selected for demodulation and regeneration relay without using any forward error correction (FEC). Only one relay is allowed to process the received signals at one time based on the symbol-wise DF relaying method. Based on the best path selection scheme, a cooperative path is chosen to implement the transmission of the digital signal from the source node to the destination node.

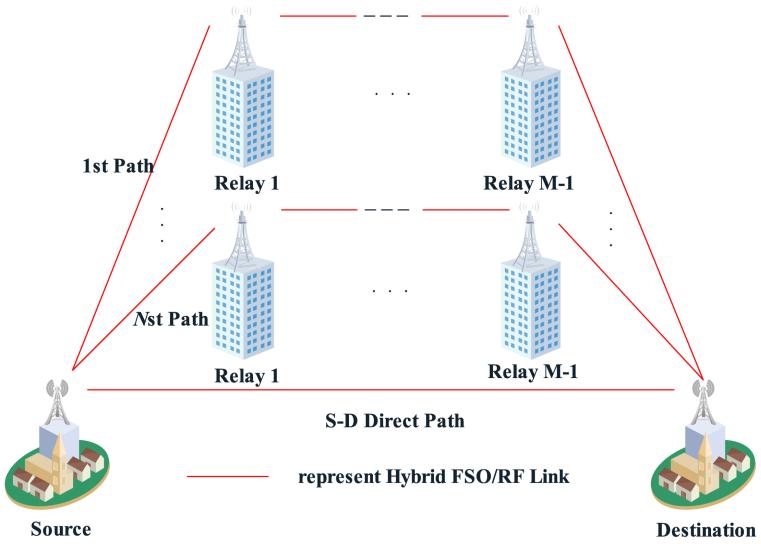

Figure 1. The schematic of the multi-hop parallel hybrid FSO/RF cooperation system.

2.1. FSO Sub-Link

Considering only Gamma–Gamma atmospheric turbulence and pointing errors, the PDF of the instantaneous SNR $\gamma_{x,y}^{FSO}$ of the FSO sub-link in any one-hop hybrid FSO/RF link (when the subscript is $(x,y)=(i,j)$, it represents the j-th hop hybrid FSO/RF link of the i-th path; when the subscript is $(x,y)=(s,d)$, it represents the direct hybrid FSO/RF link) is [21]:

$$f_{\gamma_{x,y}^{FSO}}(\gamma_{x,y}^{FSO})=\frac{\rho_{x,y}^2}{2\gamma_{x,y}^{FSO}\Gamma(\alpha_{x,y})\Gamma(\beta_{x,y})}G_{1,3}^{3,0}\left(\frac{\alpha_{x,y}\beta_{x,y}\rho_{x,y}^2}{\rho_{x,y}^2+1}\left(\frac{\gamma_{x,y}^{FSO}}{\overline{\gamma}_{x,y}^{FSO}}\right)^{\frac{1}{2}}\middle|\begin{matrix}\rho_{x,y}^2+1\\ \rho_{x,y}^2,\alpha_{x,y},\beta_{x,y}\end{matrix}\right) \tag{1}$$

where $\overline{\gamma}_{x,y}^{FSO}$ is the average SNR of one-hop FSO sub-link, $\Gamma(\cdot)$ is a Gamma function, $G(\cdot)$ is a Meijer-G function, $\rho_{x,y}$ is the ratio of the equivalent beam radius of the receiver plane to the jitter standard deviation of the receiver plane. $\alpha_{x,y}$ is a positive parameter, which is related to the effective number of large-scale vortices in the scattering process, and $\beta_{x,y}$ is a quantity related to the attenuation parameter. Assuming that the beam is a spherical wave, $\alpha_{x,y}$ and $\beta_{x,y}$ can be given by the following Equations [23]:

$$\alpha_{x,y}=\left[\exp\left(\frac{0.49\sigma_{x,y}^2}{\left(1+0.18d_{x,y}^2+0.56\sigma_{x,y}^{12/5}\right)^{7/6}}\right)-1\right]^{-1} \tag{2}$$

$$\beta_{x,y}=\left[\exp\left(\frac{0.51\sigma_{x,y}^2\left(1+0.69\sigma_{x,y}^{12/5}\right)^{-5/6}}{\left(1+0.9d_{x,y}^2+0.62d_{x,y}^2\sigma_{x,y}^{12/5}\right)^{5/6}}\right)-1\right]^{-1} \tag{3}$$

where $d_{x,y}=\left(kD^2/4L_{x,y}\right)^{1/2}$, Rytov variance $\sigma_{x,y}^2=0.5C_n^2k^{7/6}L_{x,y}^{11/6}$, $k=2\pi/\lambda^{FSO}$ is the wave number, λ^{FSO} is the optical wavelength of FSO link, D is the diameter of receiver aperture, $L_{x,y}$ is the one-hop link length, and C_n^2 is the refractive index structure constant ($m^{-2/3}$). Integrate Equation (1) according to the formula $F_{\gamma_{x,y}^{FSO}}=\int_0^{\gamma_{x,y}^{FSO}}f_{\gamma_{x,y}^{FSO}}(\gamma_{x,y}^{FSO})d\gamma_{x,y}^{FSO}$, and the CDF of $\gamma_{x,y}^{FSO}$ can be expressed as:

$$F_{\gamma_{x,y}^{FSO}}(\gamma_{x,y}^{FSO})=B_{x,y}G_{3,7}^{6,1}\left(A_{x,y}\frac{\gamma_{x,y}^{FSO}}{\overline{\gamma}_{x,y}^{FSO}}\middle|\begin{matrix}C_{x,y}\\ D_{x,y}\end{matrix}\right) \tag{4}$$

where $B_{x,y} = \frac{2^{\alpha_{x,y}+\beta_{x,y}-3}\rho_{x,y}^2}{\pi\Gamma(\alpha_{x,y})\Gamma(\beta_{x,y})}$, $A_{x,y} = \left(\frac{\alpha_{x,y}\beta_{x,y}\rho_{x,y}^2}{4(\rho_{x,y}^2+1)}\right)^2$, $D_{x,y} = \frac{\rho_{x,y}^2}{2}, \frac{\rho_{x,y}^2+1}{2}, \frac{\alpha_{x,y}}{2}, \frac{\alpha_{x,y}+1}{2}, \frac{\beta_{x,y}}{2}, \frac{\beta_{x,y}+1}{2}, 0$ and $C_{x,y} = 1, \frac{\rho_{x,y}^2+1}{2}, \frac{\rho_{x,y}^2+2}{2}$.

2.2. RF Sub-Link

Compared with the Rayleigh distribution and Rician distribution, the Nakagami-*m* distribution is more consistent with the experimental data. Therefore, the Nakagami-*m* distribution is selected as the RF fading channel in this section. The PDF of the output instantaneous SNR $\gamma_{x,y}^{RF}$ of the RF sub-link (Nakagami-*m* channel) in any one-hop hybrid link is [16]:

$$\begin{aligned} f_{\gamma_{x,y}^{RF}}(\gamma_{x,y}^{RF}) &= \left(\frac{m_{x,y}}{\overline{\gamma}_{x,y}^{RF}}\right)^{m_{i,j}} \frac{\gamma^{m_{x,y}-1}}{\Gamma(m_{x,y})} \exp\left(-\frac{m_{x,y}\gamma_{x,y}^{RF}}{\overline{\gamma}_{x,y}^{RF}}\right) \\ &= \left(\frac{m_{x,y}}{\overline{\gamma}_{x,y}^{RF}}\right)^{m_{x,y}} \frac{\gamma^{m_{x,y}-1}}{\Gamma(m_{x,y})} G_{01}^{1,0}\left[\frac{m_{x,y}\gamma_{x,y}^{RF}}{\overline{\gamma}_{x,y}^{RF}}\middle| \begin{matrix} - \\ 0 \end{matrix}\right] \end{aligned} \tag{5}$$

where $\overline{\gamma}_{x,y}^{RF}$ is the average SNR of one-hop RF link, $m_{x,y}$ ($m_{x,y} \geq 0.5$) is the fading parameter of one-hop RF link. The CDF of the SNR $\gamma_{x,y}^{RF}$ can be obtained by integration,

$$F_{\gamma_{x,y}^{RF}}(\gamma_{x,y}^{RF}) = \frac{1}{\Gamma(m_{x,y})} G_{12}^{1,1}\left(\frac{m_{x,y}\gamma_{x,y}^{RF}}{\overline{\gamma}_{x,y}^{RF}}\middle| \begin{matrix} 1 \\ m_{x,y}, 0 \end{matrix}\right) \tag{6}$$

2.3. One-Hop Hybrid FSO/RF Link Based on Selective Combination Scheme

In one-hop hybrid FSO/RF link, the selective combination scheme is adopted, which is realized by comparing the SNR of the two link signals and outputting the signal with the maximum SNR. Therefore, the output SNR $\gamma_{x,y}^{SC}$ of the selective combiner on the one-hop hybrid link can be expressed as [28]:

$$\gamma_{x,y}^{SC} = \max(\gamma_{x,y}^{FSO}, \gamma_{x,y}^{RF}) \tag{7}$$

Therefore, the CDF of the SNR $\gamma_{x,y}^{SC}$ can be expressed as [28]:

$$F_{\gamma_{x,y}^{SC}}(\gamma) = \Pr(\max(\gamma_{x,y}^{FSO}, \gamma_{x,y}^{RF}) \leq \gamma) = \Pr(\gamma_{x,y}^{FSO} \leq \gamma, \gamma_{x,y}^{RF} \leq \gamma) = F_{\gamma_{x,y}^{FSO}}(\gamma) F_{\gamma_{x,y}^{RF}}(\gamma) \tag{8}$$

It is assumed that the fading parameters on all RF paths are the same—that is, $m_{i,j} = m_{s,d} = m^{RF}$. By substituting Equations (4) and (6) into Equation (8), the CDF of the output SNR $\gamma_{x,y}^{SC}$ of one-hop hybrid sub-link can be obtained:

$$F_{\gamma_{x,y}^{SC}}(\gamma) = \frac{B_{x,y}}{\Gamma(m^{RF})} G_{12}^{1,1}\left(\frac{m^{RF}\gamma}{\overline{\gamma}_{x,y}^{RF}}\middle| \begin{matrix} 1 \\ m^{RF}, 0 \end{matrix}\right) G_{3,7}^{6,1}\left(\frac{A_{x,y}\gamma}{\overline{\gamma}_{x,y}^{FSO}}\middle| \begin{matrix} C_{x,y} \\ D_{x,y} \end{matrix}\right) \tag{9}$$

According to formula (07.34.16.0003.01) in Ref. [33], the product of two Meijer-G functions in Equation (9) can be replaced by the extended generalized bivariate Meijer's G-Function (EGBMGF),

$$F_{\gamma_{x,y}^{SC}}(\gamma) = \frac{B_{x,y}}{\Gamma(m^{RF})} G_{0,0:1,2;3,7}^{0,0:1,1;6,1}\left(\begin{matrix} 1 \\ m^{RF}, 0 \end{matrix}\middle| \begin{matrix} C_{x,y} \\ D_{x,y} \end{matrix}\middle| \frac{m^{RF}\gamma}{\overline{\gamma}_{x,y}^{RF}}, \frac{A_{x,y}\gamma}{\overline{\gamma}_{x,y}^{FSO}}\right) \tag{10}$$

3. The End-to-End Performance Analysis of the System

For the multi-hop parallel hybrid FSO/RF cooperative system based on the DF scheme, the equivalent SNR γ_{eq_i} of the ith path can be expressed as [34]:

$$\gamma_{eq_i} = \min(\gamma_{i,1}^{SC}, \gamma_{i,2}^{SC}, \cdots, \gamma_{i,M}^{SC}) \tag{11}$$

Considering the identically and independently distributed hybrid FSO/RF system, the CDF of the equivalent SNR γ_{eq_i} of the i-th path can be expressed as [34]:

$$F_{\gamma_{eq_i}}(\gamma) = 1 - \left[1 - F_{\gamma_{i,j}^{SC}}(\gamma)\right]^M \tag{12}$$

Based on the best path selection scheme, the signal with the largest SNR of the γ_{eq_i} ($i = 1, \ldots, N$ represent i-th path) and $\gamma_{s,d}^{SC}$ (the instantaneous SNR of the direct hybrid link between the source and the destination) is selected. Therefore, the equivalent output SNR γ_{eq} at the destination node can be expressed as:

$$\gamma_{eq} = \max(\gamma_{s,d}^{SC}, \gamma'_{eq}) \tag{13}$$

where $\gamma'_{eq} = \max\limits_{i=1,\ldots N} \gamma_{eq_i}$.

Assuming that FSO and RF links in all relay links have the same average SNR—that is, $\overline{\gamma}_{i,j}^{FSO} = \overline{\gamma}^{FSO}$ and $\overline{\gamma}_{i,j}^{RF} = \overline{\gamma}^{RF}$, the CDF of γ'_{eq} is:

$$\begin{aligned} F_{\gamma'_{eq}}(\gamma) &= \left[F_{\gamma_{eq_i}}(\gamma)\right]^N = \left[1 - \left[1 - F_{\gamma_{i,j}^{SC}}(\gamma)\right]^M\right]^N \\ &= \left[1 - \left[1 - \frac{B_{i,j}}{\Gamma(m^{RF})} G_{0,0:1,1:6,1}^{0,0:1,1:6,1}\left(\begin{array}{c|c} 1 & C_{i,j} \\ m^{RF}, 0 & D_{i,j} \end{array} \middle| \frac{m^{RF}\gamma}{\overline{\gamma}^{RF}}, \frac{A_{i,j}\gamma}{\overline{\gamma}^{FSO}}\right)\right]^M\right]^N \end{aligned} \tag{14}$$

Therefore, according to Equation (10) and Equation (14), the CDF $F_{\gamma_{eq}}$ of the output SNR of the destination node is

$$\begin{aligned} F_{\gamma_{eq}}(\gamma) &= F_{\gamma_{s,d}^{SC}}(\gamma) \times F_{\gamma'_{eq_i}}(\gamma) = F_{\gamma_{s,d}^{SC}}(\gamma) \times \left[1 - \left[1 - F_{\gamma_{i,j}^{SC}}(\gamma)\right]^M\right]^N \\ &= \frac{B_{s,d}}{\Gamma(m^{RF})} G_{0,0:1,1:6,1}^{0,0:1,1:6,1}\left(\begin{array}{c|c} 1 & C_{s,d} \\ m^{RF}, 0 & D_{s,d} \end{array} \middle| \frac{m^{RF}\gamma}{\overline{\gamma}_{s,d}^{RF}}, \frac{A_{s,d}\gamma}{\overline{\gamma}_{s,d}^{FSO}}\right) \\ &\times \left[1 - \left[1 - \frac{B_{i,j}}{\Gamma(m^{RF})} G_{0,0:1,1:6,1}^{0,0:1,1:6,1}\left(\begin{array}{c|c} 1 & C_{i,j} \\ m^{RF}, 0 & D_{i,j} \end{array} \middle| \frac{m^{RF}\gamma}{\overline{\gamma}^{RF}}, \frac{A_{i,j}\gamma}{\overline{\gamma}^{FSO}}\right)\right]^M\right]^N \end{aligned} \tag{15}$$

3.1. Average Bit Error Rate

For the multi-hop parallel hybrid FSO/RF system, two binary modulation scheme is used for data transmission in any FSO or RF link. According to Refs. [20,35], the mathematical expression of the average bit error rate (ABER) can be expressed as:

$$P_b = \frac{q^p}{2\Gamma(p)} \int_0^\infty \exp(-q\gamma)(\gamma)^{p-1} F_\gamma(\gamma) d\gamma \tag{16}$$

where p and q are used to describe the ABER parameters of different binary modulation schemes, as shown in Table 1.

Table 1. Parameters p and q for various binary modulation scheme.

Binary Modulation Scheme	p	q
Coherent binary phase shift keying (CBPSK)	0.5	1
Differential binary phase shift keying (DBPSK)	1	1

Substituting Equation (15) into Equation (16), the end-to-end ABER of the multi-hop parallel hybrid FSO/RF system with structure (N, M) is obtained where N is the total number of paths and M is the total number of hops of each path:

$$P_b^{mul} = \frac{q^p B_{s,d}}{2\Gamma(p)\Gamma(m^{RF})} \int_0^\infty \exp(-q\gamma)(\gamma)^{p-1} G_{0,0:1,1:6,1}^{0,0:1,1:6,1}\left(\begin{array}{c|c|c} & 1 & C_{s,d} \\ & m^{RF}, 0 & D_{s,d} \end{array} \middle| \frac{m^{RF}\gamma}{\overline{\gamma}_{s,d}^{RF}}, \frac{A_{s,d}\gamma}{\overline{\gamma}_{s,d}^{FSO}} \right) \times \left[1 - \left[1 - \frac{B_{i,j}}{\Gamma(m^{RF})} G_{0,0:1,1:6,1}^{0,0:1,1:6,1}\left(\begin{array}{c|c|c} & 1 & C_{i,j} \\ & m^{RF}, 0 & D_{i,j} \end{array} \middle| \frac{m^{RF}\gamma}{\overline{\gamma}^{RF}}, \frac{A_{i,j}\gamma}{\overline{\gamma}^{FSO}} \right) \right]^M \right]^N d\gamma \tag{17}$$

When $q = 1$, Equation (17) can be simplified by the Generalized Gauss–Laguerre quadrature function according to Ref. [36]:

$$P_b^{mul} = \frac{B_{s,d}}{2\Gamma(p)\Gamma(m^{RF})} \sum_{t=1}^{n} H_t G_{0,0:1,1:6,1}^{0,0:1,1:6,1}\left(\begin{array}{c|c|c} & 1 & C_{s,d} \\ & m^{RF}, 0 & D_{s,d} \end{array} \middle| \frac{m^{RF} z_t}{\overline{\gamma}_{s,d}^{RF}}, \frac{A_{s,d} z_t}{\overline{\gamma}_{s,d}^{FSO}} \right) \times \left[1 - \left[1 - \frac{B_{i,j}}{\Gamma(m^{RF})} G_{0,0:1,1:6,1}^{0,0:1,1:6,1}\left(\begin{array}{c|c|c} & 1 & C_{i,j} \\ & m^{RF}, 0 & D_{i,j} \end{array} \middle| \frac{m^{RF} z_t}{\overline{\gamma}^{RF}}, \frac{A_{i,j} z_t}{\overline{\gamma}^{FSO}} \right) \right]^M \right]^N \tag{18}$$

where z_t is the t-th root of the generalized Laguerre polynomial $L_n^{(-1/2)}(z)$, the corresponding weight coefficient $H_t = \Gamma[n + (1/2)] z_t / \left\{ n!(n+1)^2 \left[L_{n+1}^{(-1/2)}(z_t) \right]^2 \right\}$, $t = 1, 2, \cdots, n$.

By substituting Equation (10) into Equation (16) and transforming it with formula (2.1) in Ref. [37], the ABER of the hybrid direct link from the source node to the destination node can be obtained:

$$P_b^{SD} = \frac{B_{s,d}}{2\Gamma(m^{RF})\Gamma(p)} G_{0,0:1,2:3,7}^{1,0:1,1:6,1}\left(p \middle| \begin{array}{c|c|c} & 1 & C_{s,d} \\ & m^{RF}, 0 & D_{s,d} \end{array} \middle| \frac{m^{RF}}{\overline{\gamma}_{s,d}^{RF}}, \frac{A_{s,d}}{\overline{\gamma}_{s,d}^{FSO}} \right) \tag{19}$$

By substituting Equation (4) into Equation (16) and transforming it with formula (07.34.21.0088.01) in Ref. [33], the ABER of the FSO-only direct link from the source node to the destination node can be obtained:

$$P_b^{FSO} = \frac{B_{s,d}}{2\Gamma(p)} G_{4,7}^{6,2}\left(\frac{A_{s,d}}{\overline{\gamma}_{s,d}^{FSO}} \middle| \begin{array}{c} 1-p, C_{s,d} \\ D_{s,d} \end{array} \right) \tag{20}$$

3.2. Outage Probability

Outage probability refers to the probability that the end-to-end output SNR is lower than a specific threshold γ_{th}. Therefore, the outage probability of the system in this paper can be expressed as [34]:

$$P_{out} = \Pr(\gamma < \gamma_{th}) = \int_0^{\gamma_{th}} f_\gamma(\gamma) d\gamma = F_\gamma(\gamma_{th}) \tag{21}$$

By substituting Equation (15) into Equation (21), it can be obtained that the end-to-end outage probability of the multi-hop parallel hybrid FSO/RF system with structure (N, M) is:

$$P_{out}^{mul} = \frac{B_{s,d}}{\Gamma(m^{RF})} G_{0,0:1,1:6,1}^{0,0:1,1:6,1}\left(\begin{matrix} 1 \\ m^{RF}, 0 \end{matrix} \middle| \begin{matrix} C_{s,d} \\ D_{s,d} \end{matrix} \middle| \frac{m^{RF}\gamma_{th}}{\overline{\gamma}_{s,d}^{RF}}, \frac{A_{s,d}\gamma_{th}}{\overline{\gamma}_{s,d}^{FSO}} \right) \times \left[1 - \left[1 - \frac{B_{i,j}}{\Gamma(m^{RF})} G_{0,0:1,1:6,1}^{0,0:1,1:6,1}\left(\begin{matrix} 1 \\ m^{RF}, 0 \end{matrix} \middle| \begin{matrix} C_{i,j} \\ D_{i,j} \end{matrix} \middle| \frac{m^{RF}\gamma_{th}}{\overline{\gamma}^{RF}}, \frac{A_{i,j}\gamma_{th}}{\overline{\gamma}^{FSO}} \right) \right]^{M} \right]^{N} \tag{22}$$

By substituting Equation (10) into Equation (21), the outage probability of the hybrid FSO/RF direct link is

$$P_{out}^{SD} = \frac{B_{s,d}}{\Gamma(m^{RF})} G_{0,0:1,1:6,1}^{0,0:1,1:6,1}\left(\begin{matrix} 1 \\ m^{RF}, 0 \end{matrix} \middle| \begin{matrix} C_{s,d} \\ D_{s,d} \end{matrix} \middle| \frac{m^{RF}\gamma_{th}}{\overline{\gamma}_{s,d}^{RF}}, \frac{A_{s,d}\gamma_{th}}{\overline{\gamma}_{s,d}^{FSO}} \right) \tag{23}$$

By substituting Equation (4) into Equation (21), the outage probability of the FSO-only direct link is

$$P_{out}^{FSO} = B_{s,d} G_{3,7}^{6,1}\left(A_{s,d}\frac{\gamma_{th}}{\overline{\gamma}_{s,d}^{FSO}} \middle| \begin{matrix} C_{s,d} \\ D_{s,d} \end{matrix} \right) \tag{24}$$

4. Results and Discussion

Under different turbulence conditions, different modulation methods, different pointing errors, different RF channel fading parameters, and different network structures, the performance of the multi-hop parallel hybrid FSO/RF cooperation system proposed in this paper is estimated, and further compared with the performance of the hybrid FSO/RF direct link and the FSO-only direct link. When the parameter n is selected as 30, the average BER of the multi-hop parallel hybrid FSO/RF system can be obtained according to Equation (18).

The structure parameters $(N = 2, M = 3)$, $(N = 2, M = 5)$, $(N = 4, M = 3)$ have been selected to avoid entanglement. Without losing generality, it is assumed that the distance between each hop and the direct link is 1 km, and the average SNR of each bit in the FSO and RF links is equal—that is, $\overline{\gamma}_{x,y}^{FSO} = \overline{\gamma}_{x,y}^{RF}$. For different turbulence intensities, FSO sub-link and channel parameters can be obtained from Tables 2 and 3, respectively[22]. Numerical results are validated by Monte Carlo simulations, and the inverse transform method was used to generate the random channel.

Table 2. FSO sub-link parameters.

Parameter	Symbol	Value
Wavelength	λ^{FSO}	1550 nm
Length of the sub-Link	$L_{x,y}$	1000 m
Receiver aperture diameter	D	0.02 m

Table 3. FSO sub-channel parameters under different turbulence intensity.

Channel Condition	$\alpha_{x,y}$	$\beta_{x,y}$	$\sigma_{x,y}^2$
Strong turbulence	2.064	1.342	3.67
Moderate turbulence	2.296	1.822	1.75
Weak turbulence	2.902	2.51	1.03

In the case of pointing errors, parameter $\rho = 6$ and RF channel fading parameter $m^{RF} = 2$, it can be seen from Figure 2 that whether CBPSK or DBPSK subcarrier modulation is used, the ABER of the FSO-only direct link is higher, while the BER of hybrid FSO/RF direct link is significantly smaller.

Therefore, hybrid FSO/RF parallel transmission can effectively improve the ABER performance of the system. Whether for FSO direct link or hybrid FSO/RF direct link, the ABER performance of the system using CBPSK modulation is better than DBPSK, and this performance difference gradually decreases with the increase of the average SNR of the receiver.

From Figure 2, we can also see that, compared with the FSO-only direct link, the ABER performance of the hybrid FSO/RF link is less sensitive to turbulence intensity—that is, the change of turbulence intensity has little impact on the ABER performance of the hybrid system. This is because the FSO link performance deteriorates rapidly with the increase of turbulence intensity, the hybrid link selects the RF sub-link signal for output. Therefore, the hybrid FSO/RF link can significantly mitigate the impact of turbulence on the BER performance.

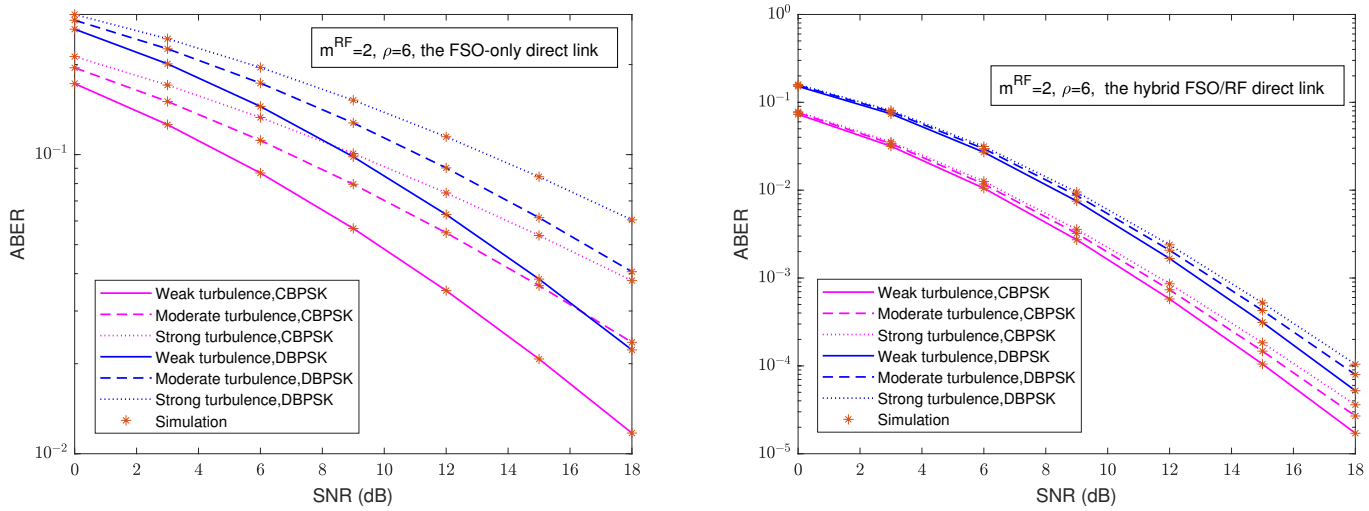

Figure 2. Influence of different modulation schemes and turbulence intensity on ABER performance of direct link. (**a**) The FSO-only direct link. (**b**) The hybrid FSO/RF direct link.

When CBPSK modulation is adopted and the pointing error parameter $\rho = 6$, Figure 3 describes the relationship between ABER and SNR of the hybrid FSO/RF direct link under different turbulence intensity and the RF fading parameter m^{RF}. Figure 3 shows that as the RF channel fading parameter m^{RF} increases, the ABER performance of the hybrid FSO/RF direct link is better.

In the case of high SNR, the increase of fading parameter m^{RF} will significantly improve the ABER performance. For example, when the average SNR of the receiver is 10 dB, compared with the case of $m^{RF} = 2$, the ABER performance of the hybrid direct link when $m^{RF} = 6$ is improved by an order of magnitude; When the average SNR of the receiver is 20 dB, compared with the case of $m^{RF} = 2$, the ABER performance of the hybrid direct link when $m^{RF} = 6$ is improved by two orders of magnitude.

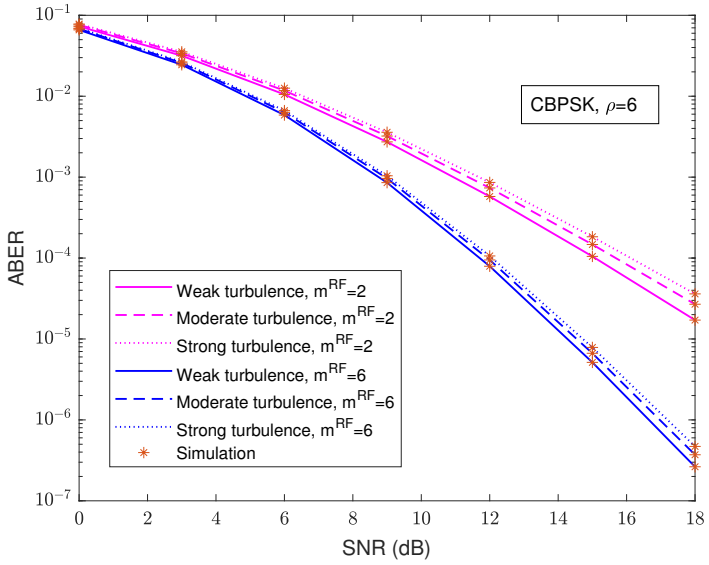

Figure 3. The ABER of the hybrid FSO/RF direct link under different turbulence intensity and RF fading parameters.

Considering the system conditions of CBPSK modulation, RF fading parameter $m^{RF} = 2$, and pointing error parameter $\rho = 6$, Figure 4 describes the relationship between the ABER and the SNR of the multi-hop parallel hybrid FSO/RF system under different relay-assisted structres and turbulence intensity. It can be seen from Figure 4 that under the same relay-assisted structure, the ABER of the multi-hop parallel hybrid system will increase with the increase of turbulence intensity. Under the same turbulence intensity, when the total number of paths N is constant, the ABER of the multi-hop parallel hybrid system will increase with the increase of the number of hops M, and when the number of hops M is constant, the ABER of the multi-hop parallel hybrid system decreases with the increase of the total number of paths N.

This is because it is assumed that the FSO and RF link channel environments of each hop are the same, and thus the ABER performance of each hop hybrid link is also the same. With the increase of hops, the transmission distance and range can be increased but the cumulative ABER of the system will also increase. Since the signal with the largest SNR is selected for output at the receiver, increasing the number of transmission paths means that the probability of the signal with large SNR received at the receiver is greater; therefore, the end-to-end BER of the system will be reduced.

When the RF link fading parameter $m^{RF} = 2$, Figure 5 shows the relationship between the ABER and the SNR of the multi-hop parallel hybrid FSO/RF system under different turbulence intensity, different relay-assisted structures, and different pointing errors. It is obvious from Figure 5 that for any turbulence intensity and pointing errors, the ABER performance of the multi-hop parallel hybrid FSO/RF system is better than that of the hybrid FSO/RF direct link, and increasing the total number of transmission paths N can significantly improve the ABER performance of the multi-hop parallel hybrid system.

In strong turbulence, the ABER of the multi-hop parallel hybrid FSO/RF system will increase rapidly with the increase of the hop number M. For example, when the output SNR of the receiver is 10 dB, for $\rho = 1$ and $\rho = 6$, the ABER of the multi-hop parallel hybrid systems $(N = 2, M = 5)$ are 2.312×10^{-4} and 1.798×10^{-4}, respectively, while the ABER of the multi-hop parallel hybrid systems $(N = 2, M = 3)$ are 1.113×10^{-4} and 8.588×10^{-5}, respectively.

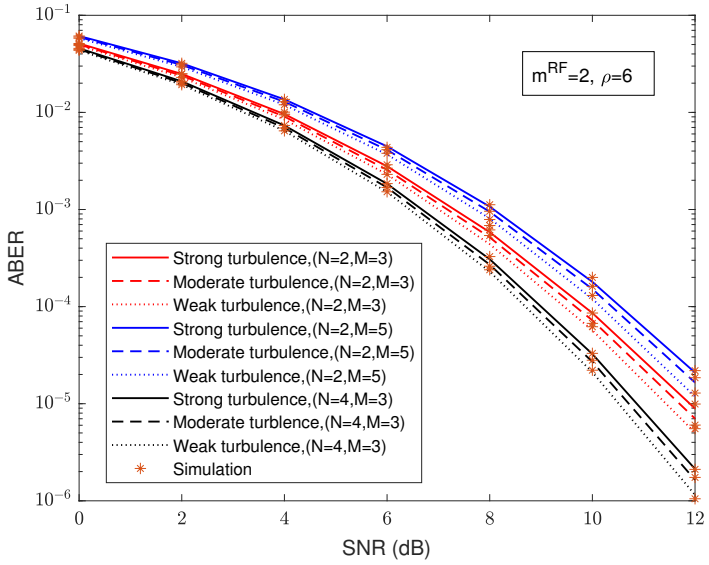

Figure 4. Relationship between the ABER and the SNR of the multi-hop parallel hybrid system under different relay-assisted structures and turbulence intensity.

In weak turbulence, the multi-hop parallel hybrid FSO/RF system is affected by the pointing errors and hop number M. For example, when the output SNR of the receiver is 10 dB, for $(N = 2, M = 5)$ and $(N = 2, M = 3)$, the ABER of the multi-hop parallel hybrid systems with $\rho = 1$ are 1.13×10^{-4} and 8.287×10^{-5}, respectively, while the ABER of the multi-hop parallel hybrid systems with $\rho = 6$ are 1.204×10^{-4} and 5.705×10^{-5}.

When the turbulence is moderate and the pointing error parameter is large, the influence of hop number M on the multi-hop parallel hybrid system is clear. For example, when the output SNR of the receiver is 10 dB, for $(N = 2, M = 5)$ and $(N = 2, M = 3)$, the ABER of the multi-hop parallel hybrid systems with $\rho = 6$ are 1.517×10^{-4} and 7.221×10^{-5}, respectively.

However, when the turbulence is moderate and the pointing error parameter is small, the influence of hop number M on the multi-hop parallel hybrid system is not significant. For example, when the output SNR of the receiver is 10 dB, for $(N = 2, M = 5)$ and $(N = 2, M = 3)$, the ABER of the multi-hop parallel hybrid systems with $\rho = 1$ are 2.033×10^{-4} and 1.864×10^{-4}, respectively.

Therefore, for strong turbulence and weak turbulence, increasing hop number (M) will significantly improve the ABER of the system, and increasing paths (N) will significantly reduce the ABER of the system; however, the multi-hop parallel hybrid system is little affected by the pointing errors in strong turbulence, while the system is significantly affected by the pointing errors in weak turbulence. For moderate turbulence, increasing the number of paths (N) will significantly reduce the ABER of the system; however, it is little affected by the pointing errors at this time. Furthermore, the ABER of the system will also increase when the number of hops (M) is increased.

When the fading parameter $m^{RF} = 2$ of the RF link and the FSO link is in strong turbulence, Figure 6 shows the relationship between the outage probability and the normalized SNR (U is the ratio of the specific SNR threshold to the average SNR) of the multi-hop parallel hybrid FSO/RF systems with different structures, the hybrid FSO/RF direct links and the FSO-only direct links under different pointing errors.

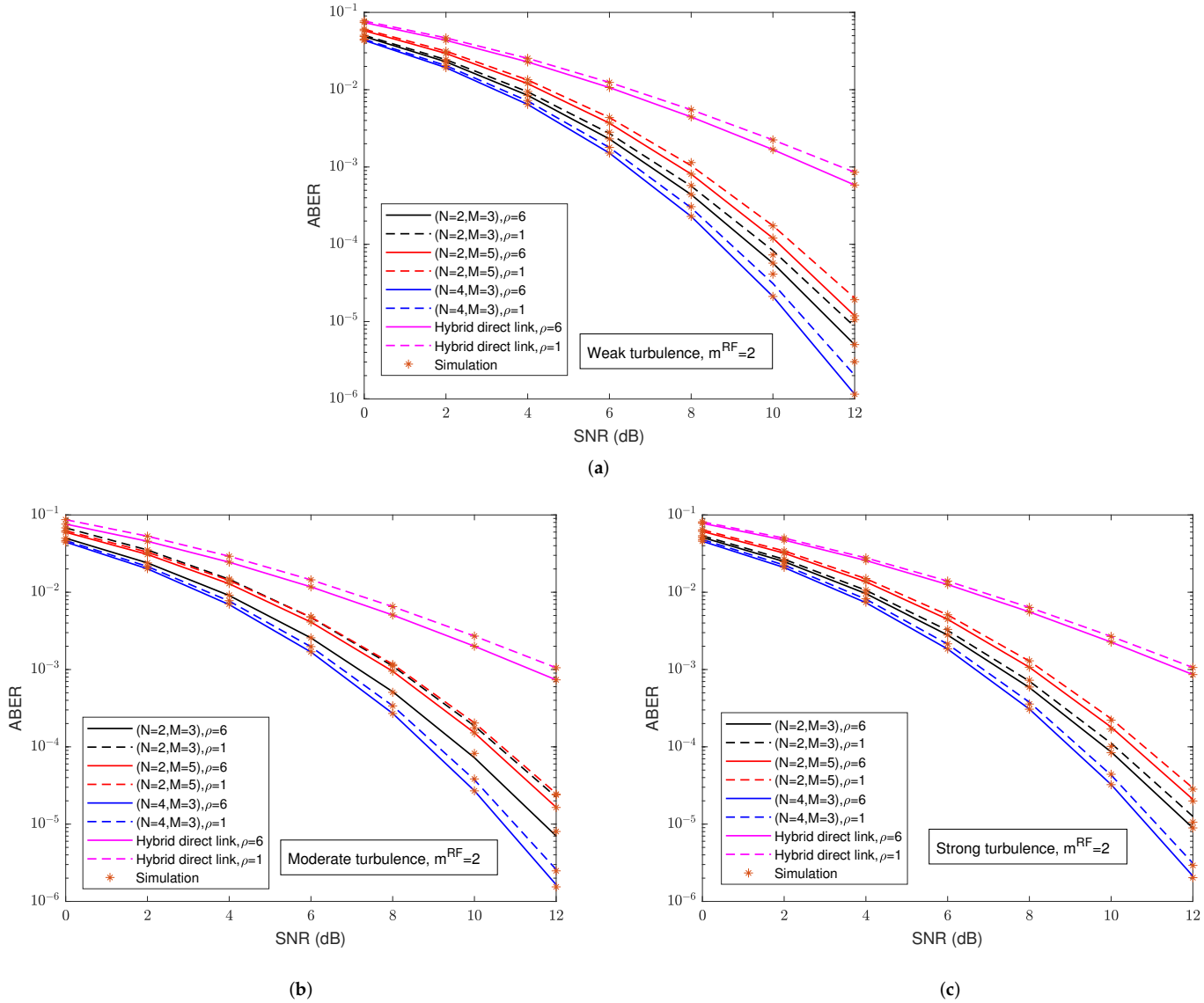

Figure 5. The relationship between ABER and SNR of the multi-hop parallel hybrid FSO/RF system and the hybrid FSO/RF direct link under different turbulence intensities, different relay-assisted structures, and different pointing errors. (**a**) weak turbulence. (**b**) Moderate turbulence. (**c**) Strong turbulence.

From Figure 6, we can see that, in the strong turbulence, as the pointing error parameter ρ increases, the outage probability of the multi-hop parallel hybrid FSO/RF systems with different structures, the hybrid FSO/RF direct links, and the FSO-only direct links will decrease. No matter how the pointing errors changes, the outage probability of the FSO-only direct link is the largest, followed by the hybrid FSO/RF parallel transmission link, and the outage probability of the multi-hop parallel hybrid FSO/RF system $(N = 4, M = 3)$ is the smallest.

In the multi-hop parallel hybrid FSO/RF system, the outage performance of the system decreases with the increase of hops, and the outage performance of the system can be improved with the increase of the number of paths. Compared with the hybrid FSO/RF direct link and the FSO-only direct link, the multi-hop parallel hybrid FSO/RF system has the best outage performance. The analytical results are well matched with the MC simulations presented in all figures.

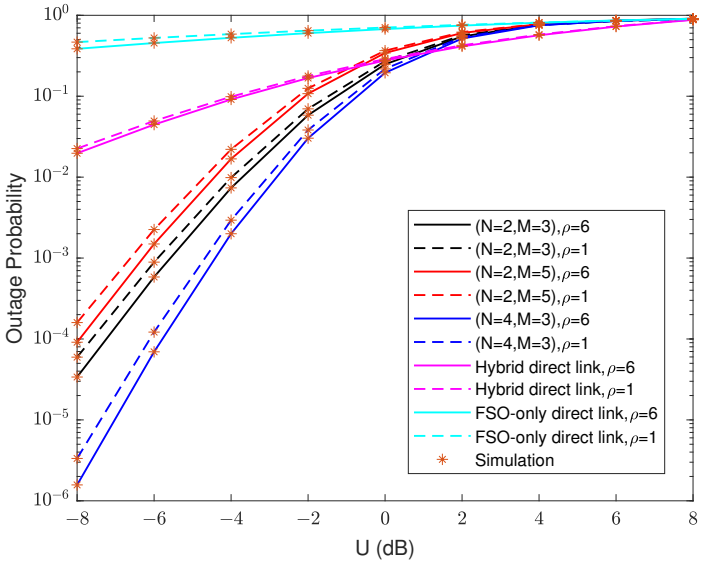

Figure 6. Relationship between outage probability and the normalized SNR of the multi-hop parallel hybrid FSO/RF system, the hybrid FSO/RF direct link, and the FSO-only direct link under different relay-assisted structures and pointing errors.

5. Conclusions

In order to improve the communication performance of the FSO system, this paper proposed a multi-hop parallel hybrid FSO/RF cooperation transmission scheme. By analyzing the end-to-end instantaneous SNR of the FSO-only direct link, the hybrid FSO/RF direct link, and the multi-hop parallel hybrid FSO/RF system, new mathematical expressions of the ABER and outage probability of them with CBPSK and DBPSK subcarrier modulation were derived. Through system simulation, the effects of turbulence intensity, pointing errors, modulation mode, and the RF fading parameter on the FSO-only direct link, the hybrid FSO/RF direct link, and the multi-hop parallel hybrid FSO/RF system were analyzed.

According to the research and analysis of this paper, we obtained some important conclusions. Affected by atmospheric turbulence and pointing errors, the transmission distance and communication performance of the multi-hop parallel hybrid FSO/RF system were the best, followed by the hybrid FSO/RF direct link, and the performance of the FSO-only direct link was the worst. For the multi-hop parallel hybrid FSO/RF system, only increasing the number of hops increased the transmission distance; however, this reduced the communication performance of the system.

By increasing the number of transmission paths, the multi-hop parallel hybrid system significantly improved the ABER and outage probability performance. The RF fading parameter m^{RF} had a great impact on the performance of the hybrid FSO/RF direct link, and the communication performance of the hybrid direct link was significantly improved when m^{RF} increased. The performance of the hybrid direct link with coherent modulation was better than that with differential modulation.

Author Contributions: Conceptualization, Y.W. and D.K.; methodology, Y.W. and G.L.; software, Y.W. and J.G.; validation, Y.W. and J.C.; formal analysis, Y.W.; writing—original draft preparation, Y.W. and D.K.; writing—review and editing, Y.W. and D.K.; supervision, D.K. All authors have read and agreed to the published version of the manuscript.

Funding: This research was funded by National Science Foundation of China (No. U2141255) and National Science Foundation of China (No.62001333).

Institutional Review Board Statement: Not applicable.

Informed Consent Statement: Not applicable.

Data Availability Statement: Not applicable.

Conflicts of Interest: The authors declare no conflict of interest.

References

1. Al-Gailani, S.A.; Salleh, M.F.M.; Salem, A.A.; Shaddad, R.Q.; Sheikh, U.U.; Algeelani, N.A.; Almohamad, T.A. A survey of free space optics (FSO) communication systems, links, and networks. *IEEE Access* **2020**, *9*, 7353–7373. [CrossRef]
2. Magidi, S.; Jabeena, A. Free space optics, channel models and hybrid modulation schemes: A review. *Wirel. Pers. Commun.* **2021**, *119*, 2951–2974. [CrossRef]
3. Yasser, M.; Ghuniem, A.; Hassan, K.M.; Ismail, T. Impact of nonzero boresight and jitter pointing errors on the performance of M-ary ASK/FSO system over Málaga ($\mathcal{M}$) atmospheric turbulence. *Opt. Quantum Electron.* **2021**, *53*, 1–23. [CrossRef]
4. Turan, H.; Subaşi, Ö. Development of Fine Tracking Unit for Hybrid ATP Mechanism in Free-space Optical Communication. In Proceedings of the 2021 29th Signal Processing and Communications Applications Conference (SIU), Istanbul, Turkey, 9–11 June 2021; pp. 1–4.
5. Li, M.; Cvijetic, M.; Takashima, Y.; Yu, Z. Evaluation of channel capacities of OAM-based FSO link with real-time wavefront correction by adaptive optics. *Opt. Express* **2014**, *22*, 31337–31346. [CrossRef] [PubMed]
6. Wu, Y.; Mei, H.; Dai, C.; Zhao, F.; Wei, H. Design and analysis of performance of FSO communication system based on partially coherent beams. *Opt. Commun.* **2020**, *472*, 1–7. [CrossRef]
7. Zhao, J.; Zhao, S.H.; Zhao, W.H.; Liu, Y.; Li, X. Performance of mixed RF/FSO systems in exponentiated Weibull distributed channels. *Opt. Commun.* **2017**, *405*, 244–252. [CrossRef]
8. Wang, P.; Cao, T.; Guo, L.; Liu, X.; Fu, H.; Wang, R.; Yang, Y. Multihop FSO over exponentiated Weibull fading channels with nonzero boresight pointing errors. *IEEE Photonics Technol. Lett.* **2016**, *28*, 1747–1750. [CrossRef]
9. Datsikas, C.K.; Peppas, K.P.; Sagias, N.C.; Tombras, G.S. Serial free-space optical relaying communications over gamma-gamma atmospheric turbulence channels. *J. Opt. Commun. Netw.* **2010**, *2*, 576–586. [CrossRef]
10. Peppas, K.P.; Stassinakis, A.N.; Nistazakis, H.E.; Tombras, G.S. Capacity analysis of dual amplify-and-forward relayed free-space optical communication systems over turbulence channels with pointing errors. *J. Opt. Commun. Netw.* **2013**, *5*, 1032–1042. [CrossRef]
11. Balaji, K.; Prabu, K. Performance evaluation of FSO system using wavelength and time diversity over malaga turbulence channel with pointing errors. *Opt. Commun.* **2018**, *410*, 643–651. [CrossRef]
12. Song, T.; Lim, C.; Nirmalathas, A.; Wang, K. Optical Wireless Communications Using Signal Space Diversity with Spatial Modulation. *Photonics* **2021**, *8*, 468. [CrossRef]
13. Dabiri, M.T.; Sadough, S.M.S. Performance analysis of EM-based blind detection for ON–OFF keying modulation over atmospheric optical channels. *Opt. Commun.* **2018**, *413*, 299–303. [CrossRef]
14. Ismail, T.; Leitgeb, E.; Ghassemlooy, Z.; Al-Nahhal, M. Performance improvement of FSO system using multi-pulse pulse position modulation and SIMO under atmospheric turbulence conditions and with pointing errors. *IET Netw.* **2018**, *7*, 165–172. [CrossRef]
15. Jagadeesh, V.; Palliyembil, V.; Muthuchidambaranathan, P.; Bui, F.M. Free space optical communication using subcarrier intensity modulation through generalized turbulence channel with pointing error. *Microw. Opt. Technol. Lett.* **2015**, *57*, 1958–1961. [CrossRef]
16. Alathwary, W.A.; Altubaishi, E.S. On the performance analysis of decode-and-forward multi-hop hybrid FSO/RF systems with hard-switching configuration. *IEEE Photonics J.* **2019**, *11*, 1–12. [CrossRef]
17. Shrivastava, S.K.; Sengar, S.; Singh, S.P. On the effect of incorrect channel condition information on modified switching scheme of hybrid fso/rf system. *IEEE Trans. Cogn. Commun. Netw.* **2019**, *5*, 1208–1217. [CrossRef]
18. Khalid, H.; Muhammad, S.S.; Nistazakis, H.E.; Tombras, G.S. Performance analysis of hard-switching based hybrid FSO/RF system over turbulence channels. *Computation* **2019**, *7*, 28. [CrossRef]
19. Makki, B.; Svensson, T.; Eriksson, T.; Alouini, M.S. On the performance of RF-FSO links with and without hybrid ARQ. *IEEE Trans. Wirel. Commun.* **2016**, *15*, 4928–4943. [CrossRef]
20. Odeyemi, K.O.; Owolawi, P.A. Selection combining hybrid FSO/RF systems over generalized induced-fading channels. *Opt. Commun.* **2019**, *433*, 159–167. [CrossRef]
21. Touati, A.; Abdaoui, A.; Touati, F.; Uysal, M.; Bouallegue, A. On the effects of combined atmospheric fading and misalignment on the hybrid FSO/RF transmission. *J. Opt. Commun. Netw.* **2016**, *8*, 715–725. [CrossRef]
22. Shakir, W.M.R. On performance analysis of hybrid FSO/RF systems. *IET Commun.* **2019**, *13*, 1677–1684. [CrossRef]
23. Shakir, W.M.R. Performance evaluation of a selection combining scheme for the hybrid FSO/RF system. *IEEE Photonics J.* **2017**, *10*, 1–10. [CrossRef]
24. Khallaf, H.S.; Garrido-Balsells, J.M.; Shalaby, H.M.; Sampei, S. SER analysis of MPPM-Coded MIMO-FSO system over uncorrelated and correlated Gamma–Gamma atmospheric turbulence channels. *Opt. Commun.* **2015**, *356*, 530–535. [CrossRef]
25. Wang, Y.; Wang, D.; Ma, J. Performance analysis of multihop coherent OFDM free-space optical communication systems. *Opt. Commun.* **2016**, *376*, 35–40. [CrossRef]
26. Zedini, E.; Alouini, M.S. Multihop relaying over IM/DD FSO systems with pointing errors. *J. Light. Technol.* **2015**, *33*, 5007–5015. [CrossRef]

27. Zedini, E.; Alouini, M.S. On the performance of multihop heterodyne FSO systems with pointing errors. *IEEE Photonics J.* **2015**, *7*, 1–10. [CrossRef]
28. Amirabadi, M.A.; Vakili, V.T. Performance comparison of two novel relay-assisted hybrid FSO/RF communication systems. *IET Commun.* **2019**, *13*, 1551–1556. [CrossRef]
29. Chatzidiamantis, N.D.; Michalopoulos, D.S.; Kriezis, E.E.; Karagiannidis, G.K.; Schober, R. Relay selection protocols for relay-assisted free-space optical systems. *J. Opt. Commun. Netw.* **2013**, *5*, 92–103. [CrossRef]
30. Gao, Z.; Liu, H.; Ma, X.; Lu, W. Performance of multi-hop parallel free-space optical communication over gamma–gamma fading channel with pointing errors. *Appl. Opt.* **2016**, *55*, 9178–9184. [CrossRef]
31. Kashani, M.A.; Uysal, M. Outage performance and diversity gain analysis of free-space optical multi-hop parallel relaying. *J. Opt. Commun. Netw.* **2013**, *5*, 901–909. [CrossRef]
32. Wang, P.; Cao, T.; Guo, L.; Wang, R.; Yang, Y. Performance analysis of multihop parallel free-space optical systems over exponentiated Weibull fading channels. *IEEE Photonics J.* **2015**, *7*, 1–17. [CrossRef]
33. WolframsWebsite. Meijer-G. 2012. Available online: http://functions.wolfram.com/PDF/MeijerG.pdf (accessed on 1 August 2020).
34. Wang, P.; Wang, R.; Guo, L.; Cao, T.; Yang, Y. On the performances of relay-aided FSO system over M distribution with pointing errors in presence of various weather conditions. *Opt. Commun.* **2016**, *367*, 59–67. [CrossRef]
35. Ansari, I.S.; Al-Ahmadi, S.; Yilmaz, F.; Alouini, M.S.; Yanikomeroglu, H. A new formula for the BER of binary modulations with dual-branch selection over generalized-K composite fading channels. *IEEE Trans. Commun.* **2011**, *59*, 2654–2658. [CrossRef]
36. Concus, P.; Cassatt, D.; Jaehnig, G.; Melby, E. Tables for the evaluation of $\int_0^\infty x^\beta e^{-x} f(x)dx$ by Gauss–Laguerre quadrature. *Math. Comput.* **1963**, *17*, 245–256.
37. Shah, M. On generalizations of some results and their applications. *Collect. Math.* **1973**, *24*, 249–266.